

Article

A Techno-Economic Study of 100% Renewable Energy for a Residential Household in China

Zhe Lv *, Zengping Wang and Wanyu Xu

State Key Laboratory of Alternative Electrical Power System with Renewable Energy Sources, North China Electric Power University, Beijing 102206, China; wangzp1103@sina.com (Z.W.); xuwanyu@ncepu.cn (W.X.)

* Correspondence: lvzhe@ncepu.edu.cn

Received: 9 May 2019; Accepted: 28 May 2019; Published: 1 June 2019



Abstract: In the context of global warming and energy shortage, this paper discusses the techno-economic feasibility of a residential household based on 100% renewable energy in China. The energy storage life, equipment's residual value, system shortage capacity and atmospheric pollution emissions were considered comprehensively. A life cycle evaluation model based on the net present value (NPV) was built. Taking a real household as an example, the levelised cost of energy (LCOE) is 0.146 \$/kW and the unmet load is only 0.86%, which has a big economic advantage when compared with diesel generators. If grid-connected, the system can bring \$8079 in 25 years when the LCOE is -0.062 \$/kW. The effects of the allowed shortage capacity, renewable energy resources, battery price and the allowed depth of discharge on the economy and energy structure were examined. For example, due to the features of the residential load, the influence of wind resource richness is more obvious than the irradiance. The maximum depth of discharge has less impact on the economy. This paper verifies the techno-economic rationality and feasibility of 100% renewable energy for a household.

Keywords: residential household; renewable energy; techno-economic feasibility; net present value (NPV); sensitivity analysis

1. Introduction

With the consumption of a large amount of fossil fuel, various environmental problems have become increasingly severe [1,2]. Many countries, like China, need to increase their share of renewable energy in total electricity generation and optimize the existing energy structure [3,4]. Moreover, there is still 22.5% of the rural population without access to electricity in 2016 globally [5]. Since the wind/solar/battery hybrid power system (WSB-HPS) can make the most use of renewable energy [6,7] and the market price of small-capacity renewable power generation equipment has dropped significantly, it is highly possible to establish a 100% renewable energy system for residential households [8]. So, it is worth to study the techno-economic feasibility for this system.

From the aspect of system optimization, electricity economic benefit, power supply reliability, and environmental benefit are usually considered. Petrillo et al. [9] proposed a model to minimize the cost of the system throughout the whole lifetime, taking into account purchase costs, installation costs, and equipment replacement and maintenance costs. Rodolfo et al. [10] additionally considered the capital recovery factor and used the total cost and electrical power to calculate the unit cost of energy. Li Chong et al. [11] adopted the total net present value and the levelised cost of energy to analyze the techno-economic feasibility.

The reliability of the system power supply is mainly calculated based on the amount of load exceeding the amount of power supply or its ratio of total power consumption [12–14]. In terms of the environmental benefit, many studies have focused on reducing greenhouse gases such as

carbon dioxide emitted from diesel generators in hybrid power generation systems [14–17]. There are mainly two kinds of methods to calculate capacity configuration. Mathematical programming is more suitable for single-objective optimization problems [18–20]. The heuristic algorithms, such as particle swarm algorithm and genetic algorithm, are ideal for solving nonlinear problems and multi-objective optimization [21–24]. Besides, some researchers use mixed integer linear programming to analyze [25].

In terms of system structure and economic analysis, Li Chong et al. [11] performed research on the off-grid hybrid power system in Urumqi, China. Based on HOMER software, the effects of ambient temperature, resident load, and the tilt angles of the photovoltaic (PV) component are considered. Based on a remote village in India, Sen et al. [26] used four kinds of renewable energy sources for a hybrid power system. According to different load types such as residential, agricultural, commercial, and industrial, the optimal off-grid capacity configuration is derived. Celik et al. [27] performed a new techno-economic analysis for small autonomous hybrid power system under optimization purposes. Tao et al. [28] presented a detailed feasibility study and economic analysis of a hybrid solar-wind-battery power system for an island.

To improve energy efficiency, some researchers designed a combined cooling, heating, and power (CCHP) system [23,29] or a combined heating and power (CHP) system [30,31]. However, for many households, as in China, the mainly thermal equipment, such as a water heater, is usually powered by solar thermal radiation or electricity. Moreover, the use of gas turbine will cause CO₂ emission and impose high costs of operation and maintenance [32].

Most of the research focuses on a single aspect, such as optimization target design and algorithm optimization, and lacks comprehensive study on the whole system. For example, when the system is under continuous cloudy or no wind weather conditions, the insignificance of the battery capacity will seriously affect the power supply reliability. Also, the different types of equipment need to be selected according to the load and renewable source. Different from analyzing traditional large capacity microgrid, the capacity of equipment required by a household is usually fixed and discrete. In the actual application process, some uncertainties on the energy structure need further sensitivity analysis.

To solve the above problems, this paper uses actual annual weather data to fully consider the impact of dynamics and random weather on the energy structure. The total net present value (NPV) model of the system is established by taking into account all factors as much as possible. Taking a certain region in Hangzhou, China as an example, the best 100% renewable energy structure for the household is obtained by comparing the NPV and the levelised cost of energy (LCOE). Sensitivity analysis of the NPV was carried out, and the changes of renewable energy structure under different renewable resource richness are studied, which provides a reference for the actual planning and operation.

2. Renewable Hybrid Power System

2.1. Wind Power

The wind power capture equation of the wind turbine is expressed as [33]:

$$\begin{cases} P_{wind} = \frac{\rho\pi R^5 \omega_t^3 C_p}{2\lambda^3} \\ \lambda = \frac{\omega_t R}{v} \end{cases} \quad (1)$$

where ρ is the air density (kg/m³), ω_t is impeller angular velocity (rad/s), R is impeller radius (m), v is wind speed (m/s), λ is blade top speed ratio, C_p is wind energy utilization factor. The wind power curve describes the actual output power, which is generally provided by the manufacturer under the rated condition.

$$P_{wind} = f(v) \quad (2)$$

To ensure the safety of the wind turbines, set the cut-out wind speed v_{max} . The lowest wind speed that can generate electricity is the cut-in wind speed v_{min} .

2.2. PV Power

The temperature of the photovoltaic panel is calculated by various factors [34]:

$$T_c = T_a + G_T \left(\frac{\tau\alpha}{U_L} \right) \left(1 - \frac{\eta_c}{\tau\alpha} \right) \quad (3)$$

where τ is the solar transmittance of the cover over the PV panel (%), α is the solar absorption efficiency (%), G_T is the solar radiation striking the PV panel (kW/m^2), η_c is the electrical conversion efficiency (%), U_L is the coefficient of heat transfer to the surroundings ($\text{kW/m}^2 \text{ } ^\circ\text{C}$), T_a is the ambient temperature ($^\circ\text{C}$).

The output of the PV panel is calculate as:

$$P_{PV} = Y_{PV} f_{PV} \left(\frac{G_T}{G_{T,STC}} \right) \left[1 + \alpha_p (T_c - T_{c,STC}) \right] \quad (4)$$

where Y_{PV} is the rated capacity of PV panel (kW), f_{PV} is the derating factor (%) which is usually set to 90% [35], G_T , $G_{T,STC}$ are the solar radiation on the PV panel at present and on the standard test condition, respectively (kW/m^2), α_p is the temperature coefficient ($\%/^\circ\text{C}$), $T_{c,STC}$ is the temperature under the standard test condition ($25 \text{ } ^\circ\text{C}$).

2.3. Energy Storage Battery

The energy storage battery is an essential part of the renewable distributed generation system. When the battery is charged, the state of charge of the battery is expressed as:

$$S_b(t) = S_b(t-1)(1-\sigma) + \eta_{cha} \frac{P_{ch,t}\Delta t}{Q} \quad (5)$$

When the battery is discharged, the state of charge of the battery is expressed as:

$$S_b(t) = S_b(t-1)(1-\sigma) - \frac{P_{dis,t}\Delta t}{Q\eta_{dis}} \quad (6)$$

where η_{cha} , η_{dis} are the charge and discharge efficiency of the energy storage battery, respectively, σ is the self-discharge effect of battery, $P_{ch,t}$ and $P_{dis,t}$ are battery charge and discharge power, respectively, Q is nominal battery capacity (Ah).

The number of times that the battery is charged and discharged, the depth of discharge and the output power of the battery can affect the life of the battery. In this paper, the cumulative damage model is used to characterize the life of the battery. That is the total releasable power during the battery lifetime [36,37].

$$Q_{life} = f \cdot DOD \left(\frac{QV_{nom}}{1000W/kW} \right) \quad (7)$$

where Q_{life} is the battery life capacity (kWh), f is the number of failure cycles, DOD is the deep of discharge (%), V_{nom} is the battery rated voltage (V). Each discharge action can be converted into a discharge amount at a standard discharge depth. When the total accumulated discharge amount reaches the battery life capacity, it is considered to be replaced.

2.4. Others

To enhance the randomness and authenticity of the data, the volatility α is set according to the load conditions of working days and weekends in different months of the year. The hourly load data can be multiplied by α .

$$\alpha = 1 + \delta_d + \delta_h \quad (8)$$

where δ_d is the daily disturbance coefficient, δ_h is the hourly disturbance coefficient. These coefficients are extracted from a normal distribution respectively, of which the mean and standard deviation are zero.

3. System Economic Model

3.1. System Net Present Value and Levelised Cost of Energy

The net present value (NPV) of the system is to convert all income and expenses incurred during the life of the project to the present value according to the actual interest rate [25], which can be written as:

$$C_{NPV} = \frac{C_{ann,tot}}{CRF(i, R_{proj})} \quad (9)$$

where $C_{ann,tot}$ is the system annual total cost (\$/year), i is the real interest rate, R_{proj} is the system working years. For the convenience of calculation, $CRF(i, R)$ is defined as the ratio parameter to calculate the present value of an annuity. The calculation formula is as follows:

$$CRF(i, R) = \frac{i(1+i)^R}{(1+i)^R - 1} \quad (10)$$

The annual average total cost $C_{ann,tot}$ is calculated as:

$$C_{ann,tot} = \sum_{i=1}^P (C_{acap,i} + C_{arep,i} + C_{aO\&M,i}) + C_{other} \quad (11)$$

where $C_{acap,i}$ is the annual purchase cost of device i (\$/year), $C_{arep,i}$ is the annual replacement cost of device i (\$/year), $C_{aO\&M,i}$ is the annual operation and maintenance cost of device i (\$/year), C_{other} is other annual cost. The calculation formula for each part is as follows:

$$C_{acap} = C_{cap} \times CRF(i, R_{proj}) \quad (12)$$

where C_{cap} is the initial purchase cost of the equipment.

$$C_{arep} = C_{rep} \frac{CRF(i, R_{proj})}{CRF(i, R_{rep})} SFF(i, R_{comp}) - S \cdot SFF(i, R_{proj}) \quad (13)$$

$$S = C_{rep} \frac{R_{rem}}{R_{comp}} \quad (14)$$

$$SFF(i, R) = \frac{i}{(1+i)^R - 1} \quad (15)$$

where R_{comp} is the service life of the equipment, R_{rep} is the total usage time of equipment that has been replaced when the project expires. SFF is the sinking fund factor, which is a ratio used to calculate the future value of a series of equal annual cash flows. S indicates the residual value of the equipment at the end of the project lifetime, which is related to the remaining service life of the equipment R_{rem} and the replacement cost C_{rep} .

$$C_{other} = c_{cs} \cdot E_{cs} + \sum_i^k c_i M_i \quad (16)$$

where c_{cs} is the penalty factor for system capacity shortage (\$/kWh), E_{cs} is the annual capacity shortage value (kWh), c_i is the financial penalty for pollutant emissions (\$/kg), M_i is the annual emission of one particular pollutant (kg/year).

During the lifetime of the system, the levelised cost of each 1 kWh of electrical energy generated is given by [6]:

$$LCOE = \frac{C_{ann,tot}}{E_{AC} + E_{DC} + E_{sale}} \quad (17)$$

where E_{AC} is the AC load of the system, E_{DC} is the DC load of the system, E_{sale} is the amount of electricity that the system sells to the grid.

3.2. System Operation Constraint

3.2.1. Shortage Capacity Fraction Constraint

For an off-grid system, the annual shortage of electricity L_{loss} needs to be less than or equal to the maximum capacity shortage that residents can accept. The constraint is given below:

$$L_{loss} = \frac{\int_1^{8760} (P_{load,t} - P_{tot,t}) dt}{\int_1^{8760} P_{load,t} dt} \times 100\% \leq L_{max} \quad (18)$$

where $P_{load,t}$ is the load power at time t , $P_{tot,t}$ is the system output power at time t .

3.2.2. Power Balance Constraint

For a grid-connected system, the amount of power generated needs to meet the load demand at whole times to ensure the reliability of the user's electricity.

$$P_{ch,t} + P_{load,t} = P_{g,t} + P_{wind,t} + P_{PV,t} + P_{dis,t} \quad (19)$$

where $P_{ch,t}$, $P_{dis,t}$ are the battery charge and discharge power, respectively, $P_{wind,t}$, $P_{PV,t}$, $P_{g,t}$ are the wind turbine power, the PV power and the power purchased from the grid, respectively.

3.2.3. Contact Line Power Constraint

For a grid-connected system, there are upper and lower limits on the transmission power between the grid side and the system. The charging and discharging power of the battery is limited by the device itself.

$$P_{g,min} \leq P_{g,t} \leq P_{g,max} \quad (20)$$

3.2.4. Energy Storage Battery Constraint

The charging and discharging power of the battery is limited.

$$0 \leq P_{ch,t} \leq P_{ch,max} \quad (21)$$

$$0 \leq P_{dis,t} \leq P_{dis,max} \quad (22)$$

where $P_{ch,max}$ and $P_{dis,max}$ are the physical bounds of the charge/discharge power.

To prevent irreversible damage caused by overcharge/undercharge, the $S_b(t)$ is restricted by:

$$S_{b,min} \leq S_{b,t} \leq S_{b,max} \quad (23)$$

where $S_{b,min}$ and $S_{b,max}$ are the lower and upper bounds of the state of battery, respectively.

4. Input Data Analysis

4.1. Renewable Resources

This paper takes a general household (120.1° E, 30.3° N) in Zhejiang Province as the research case. The renewable resource data obtained through the Meteorological Data Centre of China Meteorological Administration is shown in Figure 1. The local surface roughness is 0.1 m and the elevation is 97 m. When the actual data wind speed is not fine enough, the Weibull k -value, the autocorrelation factor [38,39] should be considered to describe the wind speed further. According to statistics, the cumulative time of wind speed over 3 m/s in this area is about 5500 h, and the annual average daily radiation intensity is 4.07 kWh/m².

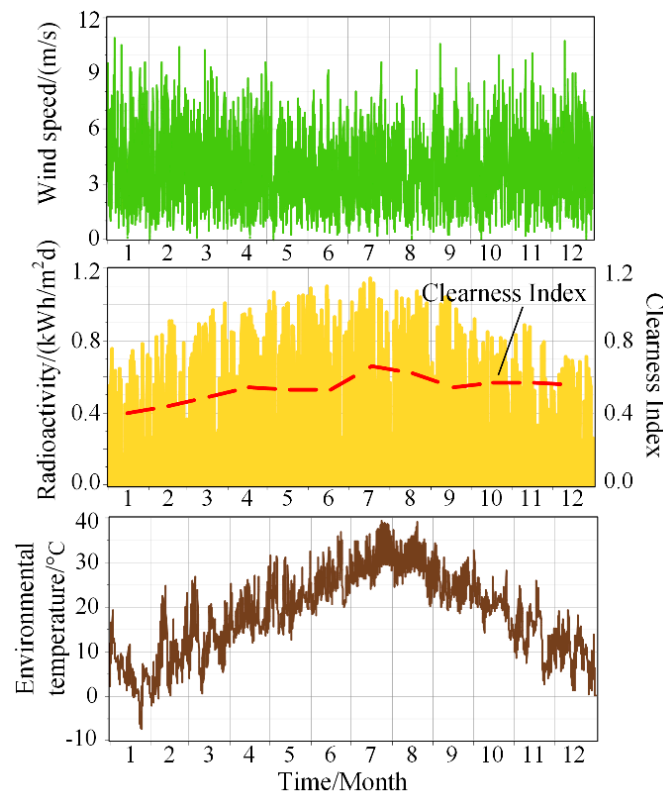


Figure 1. Year-round weather data of a certain area in Hangzhou.

4.2. Pollution and Punishment Standards

The WSB-HPS is different from traditional thermal power generation and has an apparent environmental benefit. Therefore, a quantitative analysis of its environmental value is required. For the grid-connected system, the electricity purchased from the grid is usually from thermal power generation. The emission coefficient (conventional subcritical coal-fired power plant) and environmental value in China are shown in Table 1 [40].

Table 1. Thermal power plant pollutant emission coefficient and environmental value standard.

Emissions	CO ₂	CO	SO ₂	N	TSP
Emission coefficient (g/kWh)	822	0.12	8.55	3.80	0.19
Environmental value (\$/kg)	0.0043	0.181	1.087	1.45	0.399

4.3. Selection of System Equipment

4.3.1. Photovoltaic Equipment

According to the design specifications of PV power station [23], under the off-grid situation, the inclination angle needs to ensure that the photovoltaic panel receives the largest amount of irradiation at the lowest irradiance month, which is selected as 53.5°. Under the grid-connected operation, the inclination angle needs to ensure that the photovoltaic panel receives the largest amount of annual radiation, which is selected as 26.2°.

4.3.2. Wind Turbine Equipment

The output power curves of different types of wind turbines are different. The complementary combination can improve the utilization efficiency of wind energy resources and maximize the benefits of residential residents. According to the actual wind resource condition, three types of wind turbines were selected as research objects. The output power curves of the wind turbines are shown in Figure 2.

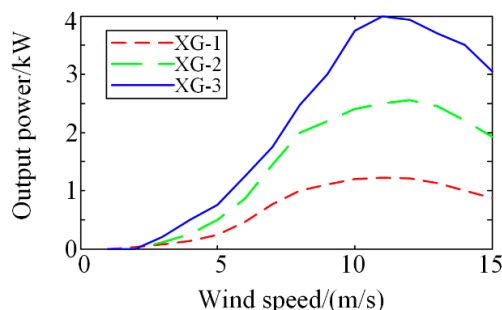


Figure 2. The output power curve of three kinds of wind turbines.

4.3.3. Energy Storage Equipment

The choice of battery capacity is related to the actual load demand and the number of autonomous days. If the energy storage capacity is insufficient, it will affect the reliability of power supply and bring adverse effects on battery life. If the energy storage capacity is excessive, the system economy will be reduced, and additional self-discharge loss will be incurred. Therefore, the average load of the maximum load month is generally selected as the measurement standard, and the number of autonomous days is set to two days. The main parameters of the equipment are shown in Table 2.

Table 2. The main parameters of the WSB-HPS equipment.

Parameter	Data	Parameter	Data
1.Battery	S-480	2.PV	CN-300
Nominal capacity	480 Ah	Nominal power	280~305 W
Nominal voltage	6 V	Standard efficiency	18.6%
Round trip efficiency	85%	Temperature coefficient	-0.39%/°C
Max. discharge depth	70%	Ground reflectance	20%
Max. charge current	18 A	Nominal operating temp.	44 °C (±2 °C)
Max. charging rate	1 A/Ah	Short-circuit current	9.72 A
Lifetime capacity	1463 kWh		
3.Wind Turbine	XG-1	XG-2	XG-3
Nominal power	1000 W	2000 W	3000 W
Rotor diameter	2.8 m	3.8 m	4.5 m
Hub height	10 m	10 m	10 m
Rated wind speed	8 m/s	8 m/s	9 m/s
Cut-in wind speed	2 m/s	2 m/s	2 m/s
Cut-out wind speed	20 m/s	20 m/s	20 m/s

4.3.4. Others

The annual interest rate of each equipment is set to 4%, the system can allow the shortage capacity ratio to be $L_{loss} = 1\%$, and the system shortage capacity penalty is 0.2 \$/kWh. According to the peak residential load described below, an inverter (GW6000) with a nominal power of 6.2 kW is selected. The maximum operating efficiency of the inverter is 98%, and the equipment capacity is selected according to the load. The economical parameters of each device in the system are shown in Table 3 [41–43]. According to the above analysis, the battery ends up due to the expiration of the service lifetime or due to the exhaustion of the life capacity.

Table 3. Economic cost and life of each equipment.

Equipment	Initial	Replacement	Operation & Maintenance	Lifetime
CN-300	\$145	\$102	\$1.45	20 years
XG1	\$421	\$361	\$3	25 years
XG2	\$780	\$668	\$5.5	25 years
XG3	\$1220	\$1045	\$8.5	25 years
GW6000	\$526	\$526	0	20 years
S-480	\$250	\$225	0	8 years

5. Case Study

Based on the real monitoring data, the load curve of a household is shown in Figure 3. The total annual electricity consumption of the household is 5935 kWh. There are three peak load times in one day, which are located at 7 am, 12 noon and 8 pm. At other times, the load is used for the indoor lighting and the standby state of electrical appliances such as refrigerators and televisions. Since there is no heating pipe in the area, it is dependent on the air conditioner for heating in winter. The simulation time is set to 1 h, and the whole lifetime of the system is set to 25 years.

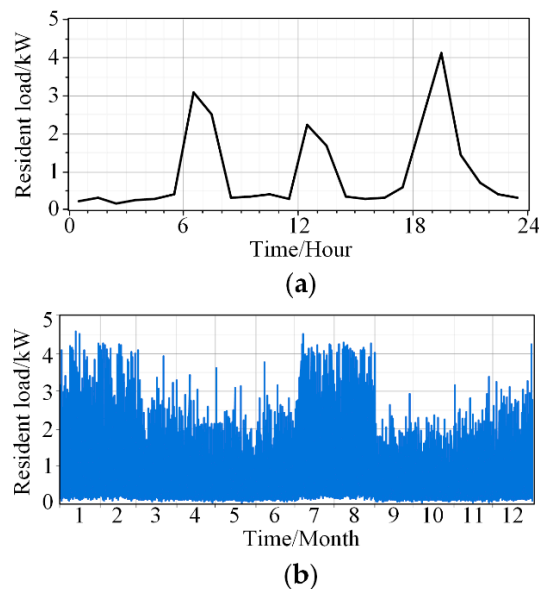


Figure 3. Load curve for a household: (a) the typical daily load curve of the household, (b) the annual load curve of the household.

The system optimal search space is set, as shown in Table 4. The capacity of PVs is from 0 to 20 kW, and the number of wind turbines is from 0 to 10. In total, there are 640,000 combinations for the household.

Table 4. Simulation system search space.

PV/kW	XG-1/No.	XG-2/No.	XG-3/No.	Battery/No.
0	0	0	0	0
1	1	1	1	4
2	2	2	2	8
20	10	10	10	32

NOTE There are a total of 640,000 ($20 \times 10^3 \times 32$) combinations.

5.1. Techno-Economic Feasibility Analysis

This paper adopts the DC bus structure. The DC bus voltage is 300 V, and the AC bus voltage is 220 V. The results of different structures in the lifetime of the system are obtained with the help of the simulation software HOMER. Furthermore, the techno-economic feasibility is analyzed in depth.

As shown in Figure 4 and Table 5, the optimal structure W-P-B (1) is obtained by comparing the system NPV and LCOE. The PV capacity is 5 kW, the wind turbine capacity is 7 kW, and the energy storage battery capacity is 34.56 kWh. According to wind speed, different types of wind turbines can be used to improve the utilization of wind. The LCOE is calculated to be \$0.146 based on the total power generation, less than two times the current price of electricity in the rural area of Zhejiang Province (\$0.08). Compared with the P-B system and the W-B system, the cost of the W-P-B (1) is reduced by 44.2% and 18.8%, respectively.

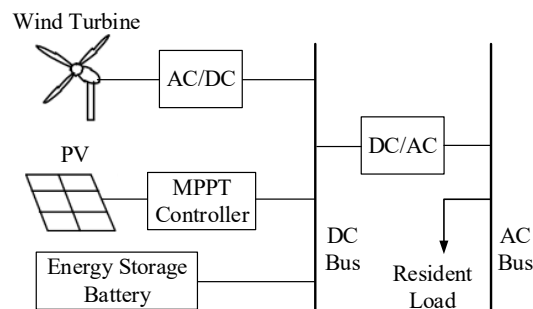


Figure 4. Composition chart of WSB-HPS, where the wind turbine, PV and the energy storage battery connected to the DC bus through respective power conversion device.

Table 5. Optimal renewable energy structure schemes.

Structure	PV/kW	XG1/No.	XG2/No.	XG3/No.	Battery/No.	LCOE/\$	NPV/\$
W-P-B (1)	5	4	0	1	12	0.146	13,548
W-P-B (2)	3	4	3	0	12	0.148	13,732
W-P-B (3)	4	0	0	3	12	0.149	13,854
W-B	0	3	0	4	16	0.180	16,689
P-B	19	0	0	0	24	0.261	24,264

NOTE W represents the wind turbine. P represents the PV. B represents the battery.

Moreover, the electricity price of diesel generators is usually between \$0.29~\$0.44, approximately two or three times of the WSB-HPS. As a result, the WSB-HPS has shown significant economic advantages in areas with abundant renewable resources and proven the feasibility of 100% renewable energy supply for residential households. Besides, it is necessary to calculate the power generation of each piece of equipment in order to ensure that the regular load demand is met. Based on this, the corresponding analysis suggestions are given.

5.1.1. System Power Generation Analysis

As shown in Table 6, the hybrid power system will waste a lot of excess electricity power (174% in this paper). If the household replaces traditional fossil energy-consuming equipment with the

electrical equipment, such as electric vehicle and electric heating system, the economic benefit can be significantly improved. Figure 5 presents the output power of PV is even lower in summer than in winter, although the irradiance in summer is higher than in winter. Because the efficiency of PV is sensitive to temperature, and in summer, the internal temperature of PV can reach more than 50 °C.

Table 6. Electrical consumption and production of the system.

Each Part of the System	Electricity/kWh	Fraction
Wind power	10,647	179%
PV power	6160	104%
Total electricity consumption	5935	100%
Excess electricity	10,306	174%
Capacity shortage	61.0	1.0%
Unmet load	51.1	0.86%

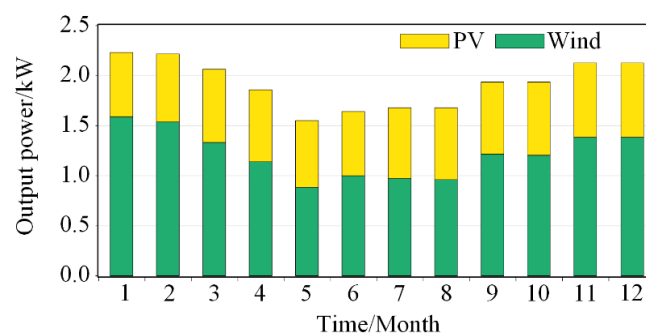


Figure 5. Daily average power in different months.

As shown in Figure 6, the inconsistency between the peak load and the peak of renewable energy leads to the charge and discharge behavior of the energy storage battery. During the daytime, solar energy is concentrated and abundant, which increases the SOC of the energy storage battery. The distribution of wind energy is more dispersed and concentrates in the morning and evening. By making full use of the coordination effect of the energy storage battery, the reliability of the resident electricity is guaranteed.

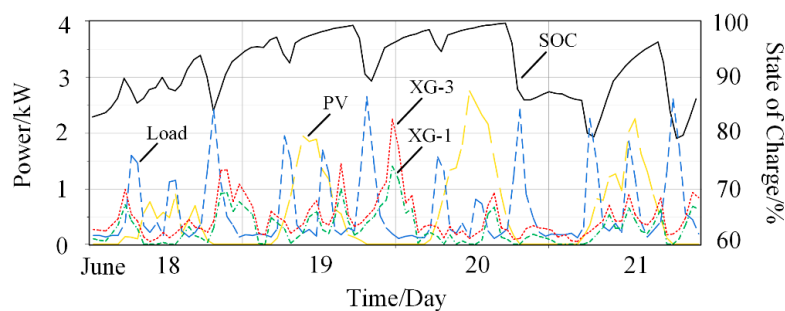


Figure 6. Power curve of WSB-HPS from June 18 to 21.

According to the statistics of Figure 7, the frequency that the state of charge (SOC) is above 60% is 94.5%. The frequency that the SOC is above 80% is 83.5%. In February and August, due to the heavy load and the maximum discharge depth of battery, there was a shortage of capacity. The maximum power shortage was 3.5 kW, and the total unmet load was 51.1 kWh, accounting for 0.86% of the total electricity consumption. Therefore, the system can use standby energy storage equipment in February and August temporarily, which will reduce battery life loss and improve power supply reliability significantly.

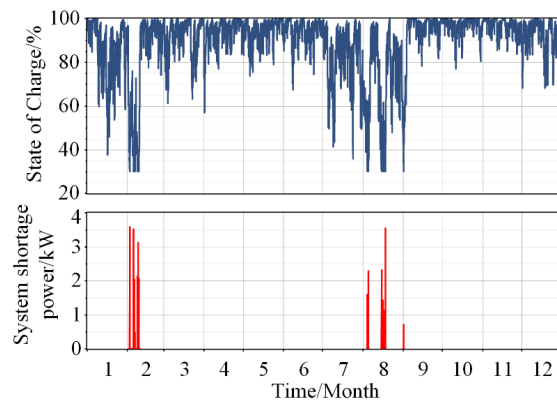


Figure 7. SOC of the battery and the system shortage power through a year.

5.1.2. Sensitivity Analysis

Sensitivity analysis is used to verify whether the best result has robustness under the allowable fluctuation range of external factors, and provide a reference for practical projects in different renewable sources. The sensitivity analysis was carried out in five aspects, which is shown in Figure 8.

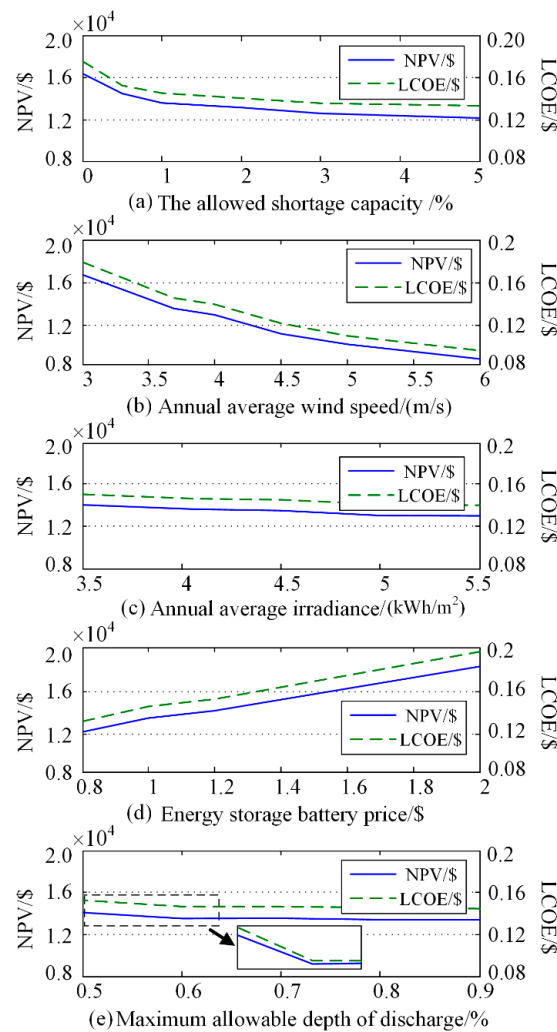


Figure 8. The sensitivity analysis of the NPV and LCOE to the allowed shortage capacity, average wind speed, average irradiance, battery price and maximum allowable depth of discharge, respectively. The changes in LOCE and NPV are basically the same.

Figure 8a shows that the NPV decreases exponentially with the increase of the allowable shortage capacity. When L_{loss} increases from 0% to 1%, the NPV decreases by 15.6%. Figure 8b,c show that the NPV decreases linearly with the increase of renewable resources richness, and the effect of wind speed is more significant than that of irradiance. Figure 8d shows that the energy storage batteries still account for a higher proportion of the total cost, compared with other equipment. The NPV of the system increases linearly with the increase in the price of the energy storage battery. Figure 8e shows that the changes of NPV and LCOE are not apparent when the maximum allowable discharge depth is set to a different value. Since the capacity shortage occurs only in a few days throughout the year, the effect of the higher discharge depth on the battery life is not obvious.

Figures 9 and 10 analyze the impact of the richness of renewable resources on the optimal energy structure. The overall trend shows that the capacity of each part of the system decreases with the increase of renewable resource richness. However, as can be seen in conjunction with Figure 6, the PV output power is mainly concentrated around noon, which can basically meet the load peak demand at noon. However, if the SOC of the battery is very high at this time, the excess solar energy will not be stored in time. This will cause much waste. The distribution of the output power of the wind turbine is more dispersed within one day, which is more similar to the residential load curve. It is beneficial to replenish the energy of the energy storage battery in time when the load is low. Therefore, the effective utilization rate of wind energy resources will be significantly larger than that of irradiance resources. Compared with the annual average irradiance, with the increase of the average annual wind speed, the capacity of each piece of power generation equipment is significantly reduced. When the average wind speed reaches 6 m/s, wind power completely replaces PV power.

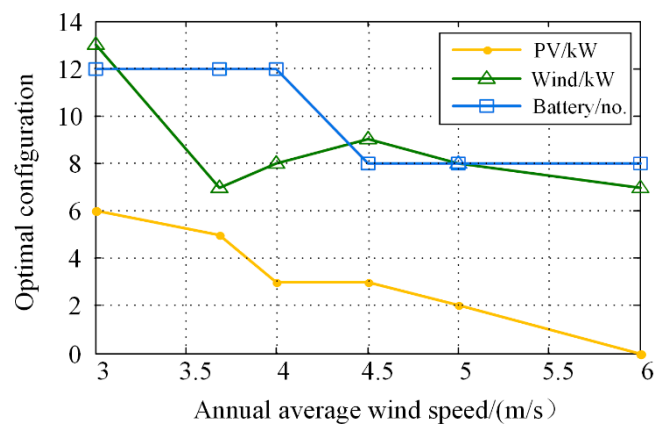


Figure 9. Relationship between optimal system configuration and wind speed.

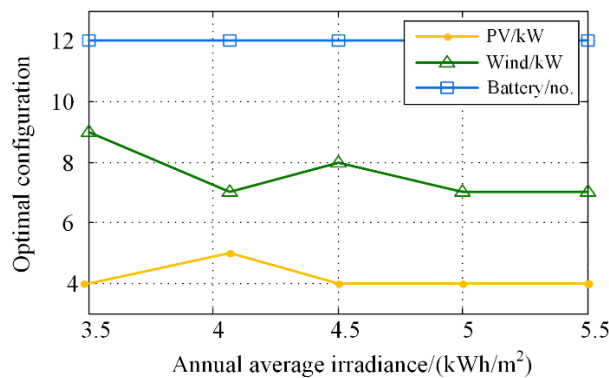


Figure 10. Relationship between optimal system configuration and irradiance.

5.2. Grid-connected System Analysis

According to the analysis of the above system, much electric power is wasted. If the WSB-HPS is connected to the grid in some conditions, the difference of the techno-economic feasibility between the systems needs to be analyzed. The grid-connected system structure is shown in Figure 11.

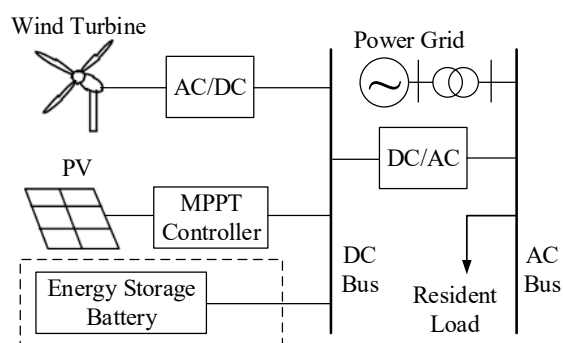


Figure 11. Diagram of grid-connected WSB-HPS. Usually the energy storage battery can be removed under the situation of grid-connected.

According to Table 7, the W-P system is still the best of different configurations for grid-connected. Compared with the 100% renewable energy system, residents can achieve \$8079 during the whole lifetime of the system. The price of the energy storage system is still higher than that of the power grid as a backup power source. As the penetration rate of renewable energy increases, the system economic benefits have increased significantly. As shown in Table 8, the emissions of atmospheric pollutants and corresponding fines are also reduced.

Table 7. Optimal structure schemes of grid-connected system.

Structure	PV/kW	XG1/no.	XG3/No.	Inverter/kW	Battery/No.	Permeability/%	LCOE/\$	NPV/\$
W-P	5	4	1	8	0	90%	−0.062	−8079
W-P-B	5	4	1	8	4	90%	−0.053	−5885
W	0	4	1	7	0	81%	−0.022	−2064
W-B	0	4	1	7	4	81%	0.001	130
P	5	0	0	7	0	60%	0.04	3703
P-B	5	0	0	6	4	60%	0.062	5790

NOTE W represents the wind turbine. P represents the PV. B represents the battery. A negative value indicates that the resident receives the corresponding income.

Table 8. Annual average savings of atmospheric pollutants.

Pollution	Emissions
CO ₂	−8532.7 (kg/year)
CO	−1.25 (kg/year)
SO ₂	−1.83 (kg/year)
NO _x	−655.3 (kg/year)
TSP	−5.91 (kg/year)

If the grid has requirements for the volatility of purchasing power, it is necessary to consider the economic benefit of energy storage. By increasing the purchase price beyond the fluctuation range as a constraint, the simulation results are shown in Figure 12. When the energy storage capacity is insufficient, the higher electricity price will increase the system NPV. When the energy storage capacity is excessive, the higher energy storage cost will increase the system NPV.

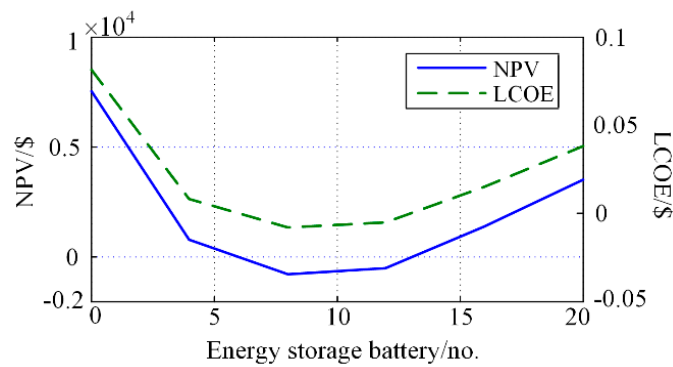


Figure 12. Relationship between energy storage capacity and system economics.

As shown in Figure 13, when the hybrid power system produces more electricity than the load consumption, the excess electricity will be sold to the grid. When renewable resources are insufficient, the power grid acts as a backup power source to sell electricity to the household. According to Table 9, only about 10% of electricity needs to be purchased from the grid.

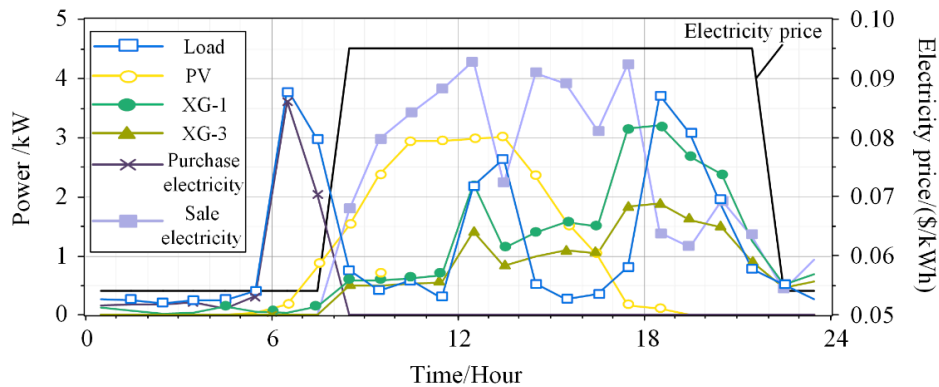


Figure 13. System power curve on July 24th. The electricity price is high from 8:00 to 22:00. At other times, the price is relatively low.

Table 9. The proportion of power generation in each part of the system.

Grid-Connected System	Electricity/kWh	Fraction
PV	6160	33%
Wind Turbine	10,647	57%
Purchase	1810	10%
Total	18,616	100%

6. Conclusions

Based on the lifecycle of the system, the techno-economic feasibility of 100% renewable energy for residential households is analyzed. For the windy areas in China, the renewable hybrid power system has a significant economic advantage compared to a diesel generator. Based on the case in this paper, the optimal energy structure contains 5 kW PV, 7 kW wind turbine, 5760 Ah battery, and a 6.2 kW convert. The levelised cost of energy of the renewable energy system is around 0.146 \$/kW. The unmet load is only 0.86% of the load consumption, which is concentrated in February and August, and the excess electricity is 174%. For the grid-connected situation, the renewable energy system can bring \$8079 in 25 years with the LCOE is -0.062 \$/kW.

The analysis results have some reference value for the actual operation planning: (1) NPV decreases exponentially with the increase of allowable shortage capacity of the system; (2) Due to the

feature of residential load, the effect of wind resource richness on the economy and capacity of the system is more significant than that of irradiance resource richness; (3) The high internal temperature of PV makes the conversion rate less than ideal in summer; (4) Changing the energy storage allowable depth of discharge within a specific range has little effect on the economy for residential household; 5) The temporary backup energy storage in high-load months can significantly improve the reliability and economy of the system.

This paper only calculates and analyses the load of a general residential household. The simulation analysis is not carried out for the case with special load requirements, such as electric vehicles. In further research, a large number of residential loads will be collected for the cluster analysis. The impact of different residential load types on the techno-economic feasibility of 100% renewable energy power system can be studied.

Author Contributions: Conceptualization, Z.L. and Z.W.; Methodology, Z.L.; Software, Z.L.; Validation, Z.L. and W.X.; Formal analysis, Z.L.; Investigation, Z.L. and W.X.; Resources, Z.L. and Z.W.; Writing—Original Draft Preparation, Z.L.; Writing—Review and Editing, W.X.; Visualization, W.X.; Supervision, Z.W.; Project Administration, Z.W.; Funding Acquisition, Z.W.

Funding: This work was supported by the National Natural Science Foundation of China (Grant No. 51637005).

Conflicts of Interest: The authors declare no conflict of interest.

Nomenclature

Abbreviations

NPV	net present value
LCOE	levelised cost of energy
WSB-HPS	wind/solar/battery-hybrid power system
SOC	state of charge
DOD	depth of discharge
PV	photovoltaic

Mathematical symbols

v	wind speed (m/s)
P_{wind}	output power of wind turbine (kW)
T_c	temperature of photovoltaic panel ($^{\circ}\text{C}$)
G_T	solar radiation striking on PV panel (kW/m^2)
P_{PV}	output power photovoltaic (kW)
α_p	temperature coefficient of PV ($\%/^{\circ}\text{C}$)
σ	the self-discharge effect of battery
η_{cha}, η_{dis}	charge and discharge efficiency
P_{ch}, P_{dis}	charge power and discharge power (kW)
Q, Q_{life}	nominal and life capacity of battery (Ah)
$S_b(t)$	the state of charge of battery (%)
f	number of failure cycles of battery
α	disturbance coefficient of load
C_{NPV}	the net present value of the system (\$)
$C_{ann,tot}$	annual total cost of the system (\$)
C_{acap}	annual purchase cost (\$)
C_{arep}	annual replacement cost (\$)
$C_{aO\&M}$	annual operation & maintenance cost (\$)
C_{other}	system's other annual cost (\$)
i	real interest rate (%)
S	residual value of the equipment (\$)
SFF	sinking fund factor
c_{cs}	capacity shortage penalty factor ($\$/\text{kWh}$)
E_{cs}	annual total capacity shortage value (kWh)
c_i	penalty for pollutant emissions ($\$/\text{kg}$)
M_i	annual emissions of the pollutants (kg/year)

CRF	ratio parameter of the present value
L_{loss}	shortage capacity fraction (%)
P_g	power of the grid (kW)
P_{load}	residential load power (kW)

References

1. Miller, R.G.; Sorrell, S.R. Introduction: The future of oil supply. *J. Phys. Chem. A* **2013**, *117*, 7737–7741.
2. Hong, S.; Bradshaw, C.J.A.; Brook, B.W. Global zero-carbon energy pathways using viable mixes of nuclear and renewables. *Appl. Energy* **2015**, *143*, 451–459. [[CrossRef](#)]
3. Almeida, M.E.; Pires, V.F.; Camilo, F.; Castro, R. Self-consumption and storage as a way to facilitate the integration of renewable energy in low voltage distribution networks. *IET Gener. Transm. Distrib.* **2016**, *10*, 1741–1748.
4. Liu, W.; Lund, H.; Mathiesen, B.V.; Zhang, X. Potential of renewable energy systems in China. *Appl. Energy* **2011**, *88*, 518–525. [[CrossRef](#)]
5. World Bank. Access to Electricity (% of Rural). Available online: <https://data.worldbank.org/indicator> (accessed on 13 January 2019).
6. Yang, H.; Wei, Z.; Lou, C. Optimal design and techno-economic analysis of a hybrid solar-wind power generation system. *Appl. Energy* **2009**, *86*, 163–169. [[CrossRef](#)]
7. Kosmadakis, I.E.; Elmasides, C.; Eleftheriou, D.; Tsagarakis, K.P. A Techno-Economic Analysis of a PV-Battery System in Greece. *Energies* **2019**, *12*, 1357. [[CrossRef](#)]
8. Bianchi, M.; Branchini, L.; Ferrari, C.; Melino, F. Optimal sizing of grid-independent hybrid photovoltaic–battery power systems for household sector. *Appl. Energy* **2014**, *136*, 805–816. [[CrossRef](#)]
9. Petrillo, A.; Felice, F.D.; Jannelli, E.; Autorino, C.; Minutillo, M.; Lavadera, A.L. Life cycle assessment (LCA) and life cycle cost (LCC) analysis model for a stand-alone hybrid renewable energy system. *Renew. Energy* **2016**, *95*, 337–355. [[CrossRef](#)]
10. Rodolfo, D.; Iván, R.C.M.; José, M.Y. Optimisation of PV-wind-diesel-battery stand-alone systems to minimise cost and maximise human development index and job creation. *Renew. Energy* **2016**, *94*, 280–293.
11. Li, C.; Ge, X.; Zheng, Y.; Xu, C.; Yang, C. Techno-economic feasibility study of autonomous hybrid wind/PV/battery power system for a household in Urumqi, China. *Energy* **2013**, *55*, 263–272. [[CrossRef](#)]
12. Kaabeche, A.; Belhamel, M.; Ibtouen, R. Sizing optimization of grid-independent hybrid photovoltaic/wind power generation system. *Energy* **2011**, *36*, 1214–1222. [[CrossRef](#)]
13. Kuznetsova, E.; Li, Y.; Ruiz, C.; Zio, E. An integrated framework of agent-based modelling and robust optimization for microgrid energy management. *Appl. Energy* **2014**, *129*, 70–88. [[CrossRef](#)]
14. Perera, A.T.D.; Attalage, R.A.; Perera, K.K.C.K.; Dassanayake, V.P.C. Designing standalone hybrid energy systems minimizing initial investment, life cycle cost and pollutant emission. *Energy* **2013**, *54*, 220–230. [[CrossRef](#)]
15. Prasad, A.R.; Natarajan, E. Optimization of integrated photovoltaic-wind power generation systems with battery storage. *Energy* **2006**, *31*, 1943–1954. [[CrossRef](#)]
16. Katsigiannis, Y.A.; Georgilakis, P.S.; Karapidakis, E.S. Multiobjective genetic algorithm solution to the optimum economic and environmental performance problem of small autonomous hybrid power systems with renewables. *IET Renew. Power Gener.* **2010**, *4*, 404–419. [[CrossRef](#)]
17. Herrando, M.; Markides, C.N.; Hellgardt, K. A UK-based assessment of hybrid PV and solar-thermal systems for domestic heating and power: System performance. *Appl. Energy* **2014**, *122*, 288–309. [[CrossRef](#)]
18. Kuznia, L.; Zeng, B.; Centeno, G.; Miao, Z. Stochastic optimization for power system configuration with renew. energy in remote areas. *Ann. Oper. Res.* **2013**, *210*, 411–432. [[CrossRef](#)]
19. Eke, R.; Kara, O.; Ulgen, K. Optimization of a wind/PV hybrid power generation system. *Int. J. Green Energy* **2005**, *2*, 57–63. [[CrossRef](#)]
20. Rubio, M.C.; Uche, M.J.; Amaya, M.G.; Angel, A.B.R. Design optimization of a polygeneration plant fuelled by natural gas and renewable energy sources. *Appl. Energy* **2011**, *88*, 449–457. [[CrossRef](#)]
21. Yang, H.; Zhou, W.; Lu, L.; Fang, Z. Optimal sizing method for stand-alone hybrid solar–wind system with LPSP technology by using genetic algorithm. *Sol. Energy* **2008**, *82*, 354–367. [[CrossRef](#)]
22. Borhanazad, H.; Mekhilef, S.; Gounder, G.V.; Modiri-Delshad, M.; Mirtaheeri, A. Optimization of micro-grid system using MOPSO. *Renew. Energy* **2014**, *71*, 295–306. [[CrossRef](#)]

23. Sharafi, M.; Elmekawy, T.Y.; Bibeau, E.L. Optimal design of hybrid renewable energy systems in buildings with low to high renewable energy ratio. *Renew. Energy* **2015**, *83*, 1026–1042. [[CrossRef](#)]
24. Zhu, J.; Li, C.; Bin, W.; Xia, L. Optimal design of a hybrid electric propulsive system for an anchor handling tug supply vessel. *Appl. Energy* **2018**, *226*, 423–436. [[CrossRef](#)]
25. Fu, B.; Ouyang, C.; Li, C.; Wang, J.; Gul, E. An Improved Mixed Integer Linear Programming Approach Based on Symmetry Diminishing for Unit Commitment of Hybrid Power System. *Energies* **2019**, *12*, 833. [[CrossRef](#)]
26. Sen, R.; Bhattacharyya, S.C. Off-grid electricity generation with renewable energy technologies in India: An application of HOMER. *Renew. Energy* **2014**, *62*, 388–398. [[CrossRef](#)]
27. Celik, A.N. Optimisation and techno-economic analysis of autonomous photovoltaic–wind hybrid energy systems in comparison to single photovoltaic and wind systems. *Energy Convers. Manag.* **2002**, *43*, 2453–2468. [[CrossRef](#)]
28. Ma, T.; Yang, H.; Lu, L. A feasibility study of a stand-alone hybrid solar–wind–battery system for a remote island. *Appl. Energy* **2014**, *121*, 149–158. [[CrossRef](#)]
29. Yan, Y.; Zhang, C.; Li, K.; Wang, Z. An integrated design for hybrid combined cooling, heating and power system with compressed air energy storage. *Appl. Energy* **2018**, *210*, 1151–1166. [[CrossRef](#)]
30. Liu, Z.; Chen, Y.; Zhuo, R.; Jia, H. Energy storage capacity optimization for autonomy microgrid considering CHP and EV scheduling. *Appl. Energy* **2017**, *210*, 1113–1125. [[CrossRef](#)]
31. Li, J.; Wang, X.; Zhang, Z.; Le, B.S.; Yang, Q.; Zhang, M. Analysis of a new design of the hybrid energy storage system used in the residential m-CHP systems. *Appl. Energy* **2017**, *187*, 169–179. [[CrossRef](#)]
32. Ogunjuyigbe, A.S.O.; Ayodele, T.R.; Akinola, O.A. Optimal allocation and sizing of PV/wind/split-diesel/battery hybrid energy system for minimizing life cycle cost, carbon emission and dump energy of remote residential building. *Appl. Energy* **2016**, *171*, 153–171. [[CrossRef](#)]
33. Karthikeyan, N.; Kalidasa, M.K.; Arun, K.S.; Rajakumar, S. Review of aerodynamic developments on small horizontal axis wind turbine blade. *Renew. Sustain. Energy Rev.* **2015**, *42*, 801–822. [[CrossRef](#)]
34. Kogarko, L.N.; Zartman, R.E. Optimal configuration assessment of renewable energy in Malaysia. *Renew. Energy* **2011**, *36*, 881–888.
35. Ropp, M.E.; Begovic, M.; Rohatgi, A. Determination of the curvature derating factor for the Georgia Tech Aquatic Center photovoltaic array. In Proceedings of the Conference Record of the Twenty Sixth IEEE Photovoltaic Specialists Conference, Anaheim, CA, USA, 29 September–3 October 1997; pp. 1297–1300.
36. Drouilhet, S.; Johnson, B.L.; Stephen, D.P.E.; Johoson, L. A battery life prediction method for hybrid power applications. In Proceedings of the AIAA 35th Aerospace Sciences Meeting and Exhibit, Reno, NV, USA, 6–9 January 1997.
37. Jenkins, D.P.; Fletcher, J.; Kane, D. Lifetime prediction and sizing of lead-acid batteries for microgeneration storage applications. *Renew. Power Gener. IET* **2008**, *2*, 191–200. [[CrossRef](#)]
38. Stevens, M.J.M.; Smulders, P.T. The estimation of the parameters of the Weibull wind speed distribution for wind energy utilization purposes. *Wind Eng.* **1979**, *3*, 132–145.
39. Brett, A.C.; Tuller, S.E. The autocorrelation of hourly wind speed observations. *J. Appl. Meteorol.* **1991**, *30*, 823–833. [[CrossRef](#)]
40. Zhu, B. Environment cost evaluation of the exhaust of thermal power generation. In Proceedings of the 12th National Conference on Atmospheric Environment, Dandong, China, 17–19 October 2005.
41. Katsigiannis, Y.A.; Georgilakis, P.S.; Karapidakis, E.S. Hybrid simulated annealing-tabu search method for optimal sizing of autonomous power systems with renewables. *IEEE Trans. Sustain. Energy* **2012**, *3*, 330–338. [[CrossRef](#)]
42. The Official Website of the Guangheguineng Company. Available online: <http://www.ghgn.vipcom.cn> (accessed on 11 January 2019).
43. The Official Website of the Xing-guang Wind Turbine Company. Available online: <http://www.qdxingguang.com> (accessed on 11 January 2019).

